

U.S. Department of the Interior
U.S. Geological Survey

Analysis of Borehole-Radar Reflection Logs from Selected HC Boreholes at the Project Shoal Area, Churchill County, Nevada

By John W. Lane, Jr., Peter K. Joesten, Greg Pohll, and Todd Mihevic

Water-Resources Investigations Report 01-4014

Prepared in cooperation with the U.S. Department of Energy

Storrs, Connecticut
2001

U.S. DEPARTMENT OF THE INTERIOR
GALE A. NORTON, Secretary

U.S. GEOLOGICAL SURVEY
Charles G. Groat, Director

The use of firm, trade, and brand names in this report is for identification purposes only and does not constitute endorsement by the U.S. Government.

For additional information write to:

Branch Chief
U.S. Geological Survey, Office of Ground Water
Branch of Geophysical Applications & Support
11 Sherman Place, U-5015
Storrs Mansfield, CT 06269
<http://water.usgs.gov/ogw/bgas>

Copies of this report can be purchased from:

U.S. Geological Survey
Branch of Information Services
Box 25286
Denver, CO 80225
<http://www.usgs.gov>

CONTENTS

Abstract	1
Introduction	1
Purpose and Scope	2
Description of the Study Area	2
Data Collection and Analysis	2
Borehole-Radar Reflection Method	2
Data Processing	5
Data Analysis and Interpretation	5
Estimation of Reflector Length	6
Reflector Quality Scores: Reflector Continuity and Orientation Confidence	7
Results of Borehole-Radar Reflection Logging at the Project Shoal Area	9
Borehole HC-2	9
Borehole HC-5	9
Borehole HC-6	12
Borehole HC-7	14
Borehole HC-8	14
Summary and Conclusions	18
References Cited	22

FIGURES

1. Map showing the location of the study area, general topography, and logged boreholes at the Project Shoal Area, Churchill County, Nevada	3
2. Conceptual diagram showing the transmitter and receiver antenna arrangement for borehole-radar reflection logging and the typical reflection patterns from planar and a point reflectors	4
3. Diagram showing how the orientation of a receiving loop antenna with respect to an impinging transmitted electromagnetic wave affects the amplitude of the signal induced on the receiving antenna	5
4. Screen capture showing the use of RADINTER software to interactively interpret borehole radar reflection logs	6
5. Diagram showing the effect of reflector orientation on reflection imaging	8
6. Radar reflection logging in borehole HC-2, Project Shoal Area	10
7. Radar reflection logging in borehole HC-5, Project Shoal Area	11
8. Radar reflection logging in borehole HC-6, Project Shoal Area	13
9. Radar reflection logging in borehole HC-7, Project Shoal Area	15
10. Radar reflection logging in borehole HC-8, Project Shoal Area	17
11. Histogram showing the distribution of interpreted borehole-radar reflectors sorted by azimuth, Project Shoal Area	19
12. Histogram showing the distribution of interpreted borehole-radar reflectors sorted by dip, Project Shoal Area	19
13. Histogram showing the distribution of interpreted borehole-radar reflectors sorted by the continuity of the reflectors, Project Shoal Area	20
14. Histogram showing the distribution of interpreted borehole-radar reflectors sorted by orientation confidence, Project Shoal Area	20
15. Lower hemisphere equal-area stereo-net showing poles of all interpreted radar reflectors, weighted by reflector length and combined reflector quality, Project Shoal Area	21

TABLES

1. Radar reflection logging parameters, Shoal Area, Churchill County, Nevada.....	9
2. Planar reflectors interpreted from 60-megahertz radar reflection log, borehole HC-2, Project Shoal Area	12
3. Planar reflectors interpreted from 60-megahertz radar reflection log, borehole HC-5, Project Shoal Area	12
4. Planar reflectors interpreted from 60-megahertz radar reflection log, borehole HC-6, Project Shoal Area	14
5. Planar reflectors interpreted from 60-megahertz radar reflection log, borehole HC-7, Project Shoal Area	16
6. Planar reflectors interpreted from 60-megahertz radar reflection log, borehole HC-8, Project Shoal Area	16

CONVERSION FACTORS AND ABBREVIATIONS

Multiply	By	To obtain
kilometer (km)	0.6214	mile
meter (m)	3.281	foot

Other abbreviations used in this report:

° , degrees
MHz, megahertz

Analysis of Borehole-Radar Reflection Logs From Selected HC Boreholes at the Project Shoal Area, Churchill County, Nevada

By John W. Lane Jr., Peter K. Joesten, Greg Pohll, and Todd Mihevic

ABSTRACT

Single-hole borehole-radar reflection logs were collected and interpreted in support of a study to characterize ground-water flow and transport at the Project Shoal Area (PSA) in Churchill County, Nevada. Radar logging was conducted in six boreholes using 60-MHz omni-directional electric-dipole antennas and a 60-MHz magnetic-dipole directional receiving antenna.

Radar data from five boreholes were interpreted to identify the location, orientation, estimated length, and spatial continuity of planar reflectors present in the logs. The overall quality of the radar data is marginal and ranges from very poor to good. Twenty-seven reflectors were interpreted from the directional radar reflection logs. Although the range of orientation interpreted for the reflectors is large, a significant number of reflectors strike northeast-southwest and east-west to slightly northwest-southeast. Reflectors are moderate to steeply dipping and reflector length ranged from less than 7 m to more than 133 m.

Qualitative scores were assigned to each reflector to provide a sense of the spatial continuity of the reflector and the characteristics of the field data relative to an ideal planar reflector (orientation score). The overall orientation scores are low, which reflects the general data quality, but also indicates that the properties of most reflectors depart from the ideal planar case. The low scores are consistent with

reflections from fracture zones that contain numerous, closely spaced, sub-parallel fractures.

Interpretation of borehole-radar direct-wave velocity and amplitude logs identified several characteristics of the logged boreholes: (1) low-velocity zones correlate with decreased direct-wave amplitude, indicating the presence of fracture zones; (2) direct-wave amplitude increases with depth in three of the boreholes, suggesting an increase in electrical resistivity with depth resulting from changes in mineral assemblage or from a decrease in the specific conductance of ground water; and (3) an increase in primary or secondary porosity and an associated change in mineral assemblage, or decrease in ground water specific conductance, was characterized in two of the boreholes below 300 m.

The results of the radar reflection logging indicate that even where data quality is marginal, borehole-radar reflection logging can provide useful information for ground-water characterization studies in fractured rock and insights into the nature and extent of fractures and fracture zones in and near boreholes.

INTRODUCTION

In October 1963, an underground nuclear test was conducted at the Project Shoal Area (PSA) in Churchill County, about 50 km southeast of Fallon, Nevada. The nuclear test was conducted as part of a research program designed to enhance the detection of

underground nuclear tests in seismically active areas (Pohll and others, 1998). Because underground nuclear tests deposit radioactive materials in the subsurface, there is a potential for radioactive materials to directly contact and contaminate ground water. At the PSA, the U.S. Department of Energy is conducting characterization studies of ground-water contamination to establish contaminant boundaries to protect human health and the environment (Pohll and others, 1998).

In support of the ground-water studies, a cooperative project was conducted by the U.S. Department of Energy and the U.S. Geological Survey under Interagency Agreement DE-A108-96NV11967. Borehole-radar reflection logging was conducted in six boreholes in the PSA to identify large fractures and fracture zones in and near the boreholes. The radar logs were analyzed and interpreted by the U.S. Geological Survey to identify planar and point reflectors near the boreholes, estimate the orientation of reflectors, determine the projection depth of the reflectors relative to the boreholes, and identify characteristics of the reflection logs that could provide information about the nature and extent of fractures and fracture zones in and near the boreholes.

Purpose and Scope

This report presents results of the analysis and interpretation of borehole-radar reflection data acquired in six boreholes at the PSA. The analysis of the radar data included determination of the location and orientation of planar and point reflectors, approximation of the length of planar reflectors, and qualitative estimation of the relative continuity and characteristics of reflectors in the field data relative to an ideal planar reflector. Results of the analysis are presented in tabular form, stereo plots, and histograms. In addition, the relative arrival time and amplitude of the direct wave traveling between the radar transmitter and receiver was analyzed. Results of the direct-wave analysis are provided in graphical form as radar velocity and amplitude logs.

Description of the Study Area

The PSA is in Churchill County, Nevada, about 50 km southeast of Fallon, Nevada (fig. 1). The regional ground-water hydrology is described by

Cohen and Everett (1963) and Glancy and Katzer (1975). The University of Nevada (1965) reported results of geologic and topographic mapping, drilling operations, geophysical surveys, hydrologic testing, and geologic core analysis. Investigations have been undertaken to characterize the hydrogeology of the PSA and the effects of the nuclear test. These studies were tabulated and summarized by Pohll and others (1998).

As described in Pohll and others (1998), the PSA is in the Sand Springs Range, a north-south trending range in Nevada's Great Basin. The Sand Springs Range is bounded by near-vertical, northeast- and northwest-trending faults. Within the range, an intrusive granitic body of Cretaceous age is surrounded by metamorphosed Paleozoic and Mesozoic marine sediments. Intermittent faulting is present in the center of the Sand Springs Range as high- to moderate-angle, northeast- and northwest-trending faults. The Project Shoal test was conducted in the granite uplift of the Sand Springs Range. Near the site, ground water is present in the fractured granite about 300 m below land surface.

DATA COLLECTION AND ANALYSIS

Borehole-Radar Reflection Method

Borehole-radar reflection methods can provide information about the extent and orientation of fracture zones intersected by a borehole and fracture zones outside of the borehole that are not penetrated by drilling. This provides information about the rocks outside the borehole that would not be provided by tools that characterize only the interior of a borehole. The ability of the method to "see" beyond the borehole can potentially provide valuable insight about the network of fractures in and near boreholes.

Borehole-radar systems and methods have been developed in the United States (Rubin and others, 1978; Wright and Watts, 1982) and in Sweden (Nilsson, 1983; Olsson and others, 1988). Single-hole radar reflection methods (using omni-directional and directional receiver antennas) have been used to detect and map fractures and fracture zones at proposed high-level nuclear waste sites (Bradley and Wright, 1987; Olsson and others, 1988, 1992a, 1992b; Sandberg and others, 1991; Holloway and others, 1992; Stevens and others, 1995) and are increasingly

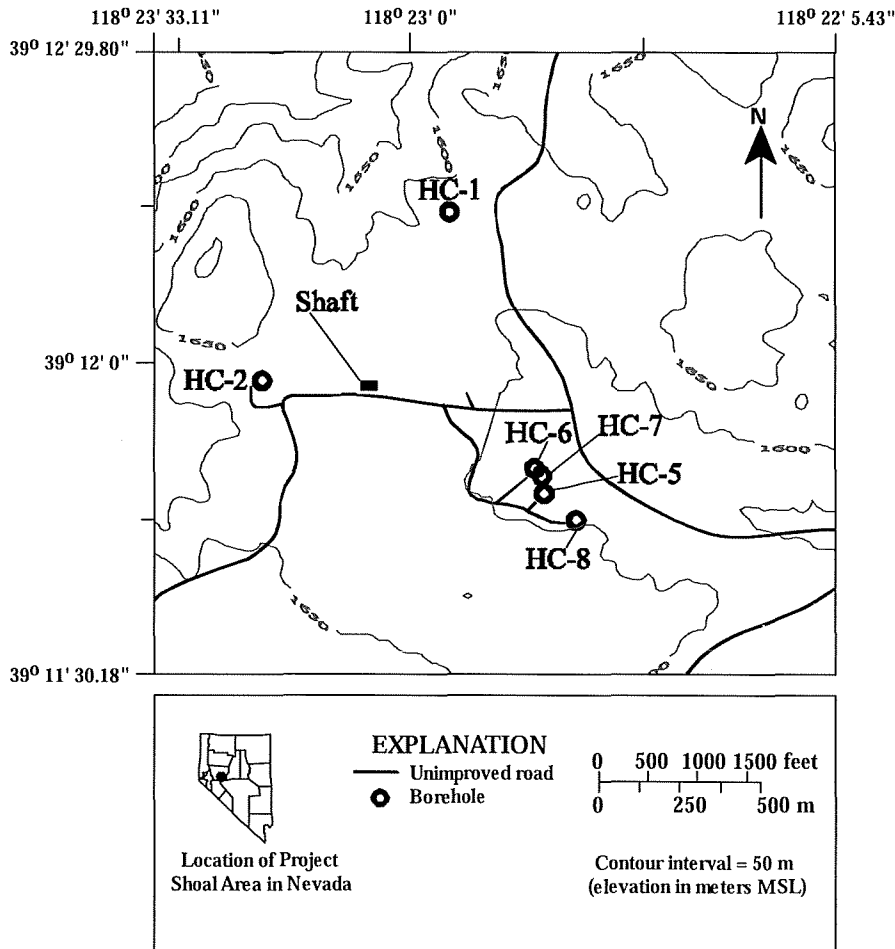


Figure 1. Location of the study area, general topography, and logged boreholes at the Project Shoal Area, Churchill County, Nevada.

utilized for ground-water investigations (Haeni and others, 1993; Gaylor and others, 1994; Lane and others, 1994; Hansen and Lane, 1995). The ABEM RAMAC borehole-radar system used for this study was developed by the Swedish Geological Survey to investigate potential high-level nuclear waste disposal sites.

Borehole-radar reflection logging is conducted by connecting a radar transmitter and receiver together as a logging tool (fig. 2). The transmitter and receiver are vertically oriented in a single borehole, and separated by a fixed distance. A high-frequency electromagnetic (EM) pulse is generated by the transmitting antenna and propagates radially into the surrounding material. Some of the energy is reflected when it encounters changes in the physical properties of the rock surrounding the borehole, such as at fractures or point-like

discontinuities. Transmitted (direct-wave) and reflected energy arriving at the receiving antenna is recorded as a function of time (fig. 2).

Reflection logging can be conducted with omni-directional or directional receiving antennas. The transmitter and the receiver antennas are moved down a single hole using a computer-controlled winch, and measurements are collected at discrete, regular intervals. The transmitter-receiver antenna separation can range from 1 to 15 m depending on the radar system, selection of antenna frequency and design, and electrical resistivity of the rock. The borehole measurement interval usually ranges from about 0.1 to 1.0 m. Omni-directional (electric-dipole) antennas provide information on the dip and depth of a reflector with respect to the borehole, but do not provide information on the orientation (strike) of a reflector. Directional receiving antennas can provide

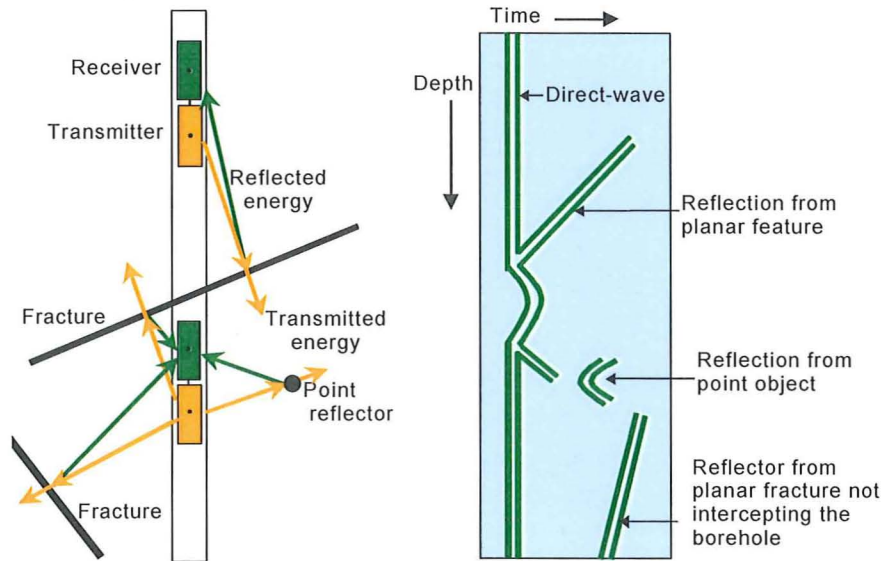


Figure 2. Transmitter and receiver antenna arrangement for borehole-radar reflection logging and the typical reflection patterns from planar and point reflectors.

information on the orientation of reflectors. The directional receiver used for this study is a magnetic-dipole type described by Falk (1992). Although the directional receiver can determine the orientation of planar reflectors and the azimuths to point reflectors, the antenna is less sensitive than the electric-dipole antenna. The radial penetration of the directional antenna used for this study is typically 50 to 70 percent that of the penetration achieved by the omni-directional antenna.

The basic principles of single-hole reflection surveying and the typical reflection patterns for planar and point reflectors, such as fractures or voids, are illustrated in figure 2. The first signal to arrive at the receiver is the direct wave, which propagates from the transmitter, through the rock, to the receiver. Due to the small diameter of most boreholes relative to the EM wavelengths used for radar reflection logging, propagation of energy along the borehole is small and limited to very high frequencies. As the transmitter and receiver antenna pair approach and pass a point scatterer, an approximately hyperbolic reflection is obtained with the apex of the hyperbola at the point closest to the borehole (fig. 2). As the transmitter and receiver antennas approach a planar reflector that intersects the borehole, the reflection travel time decreases until it merges with the direct arrival. As the transmitter and receiver pass through the

intersection location of the reflector, no reflections are obtained and a delay of the arrival time of the direct wave can occur, if, for example, the reflector is a water-filled fracture or fracture zone. As the transmitter and receiver move past the reflector intersection point, the reflection travel time increases, resulting in a two-limbed or chevron-shaped reflection pattern for a reflector that intersects the borehole (fig. 2). The reflection pattern for reflectors that do not intersect the borehole is discontinuous and displays only the upper (up-dip) or lower (down-dip) limb (fig. 2).

The EM-wave propagation velocity is required to accurately interpret the dip of planar reflectors and the radial distance to point reflectors. The EM velocity for different rock types can be roughly estimated from tabulations found in the literature (Cook, 1975), by vertical radar profiling (VRP) tests, and by analysis of the shape of the reflections from point reflectors. VRP testing is performed by fixing the transmitter location while making measurements as the receiver is moved away from the transmitter in fixed increments. The slope of the best-fit line of the transmitter-receiver distance plotted against the arrival time yields the average velocity along the borehole.

Variations in the arrival time and amplitude of the direct wave provide information about the

range of velocity and attenuation differences of the material surrounding the borehole. In resistive, saturated rocks, a delayed arrival of the direct wave (decreased velocity) coupled with a decreased pulse amplitude can indicate an increase in porosity due to fracturing; the high dielectric permittivity of water reduces EM-wave velocity.

Data Processing

For this study, signal processing of borehole-radar data was limited to (1) removal of the direct-current (DC) offset and (2) band-pass filtering (Yilmaz, 1987). The DC offset is caused by the analog-to-digital sampling electronics, which induce a drift in the signal level with time. The DC offset is removed by averaging the DC level of the first few samples of each trace before the onset of the direct arrival, and subtracting this average from the rest of the samples. Band-pass filtering is used to remove

low- and high-frequency random and system noise and other sources of noise, such as ringing induced by the impedance mismatch of the antennas with the borehole.

Data Analysis and Interpretation

Interpretation of the strike of a planar feature or the azimuth to a point reflector is performed in a manner analogous to certain methods of radio-direction finding. Using a loop antenna, it is possible to locate the radial direction to a transmitter by rotating the loop and measuring the signal induced on the receiving antenna. The magnetic component of the electromagnetic wave induces an electric current in the loop. The electromotive force in the loop is a function of the magnetic flux through the loop. Therefore, the signal induced by a plane wave is a function of the component of the variable magnetic field passing through the antenna loop (fig. 3).

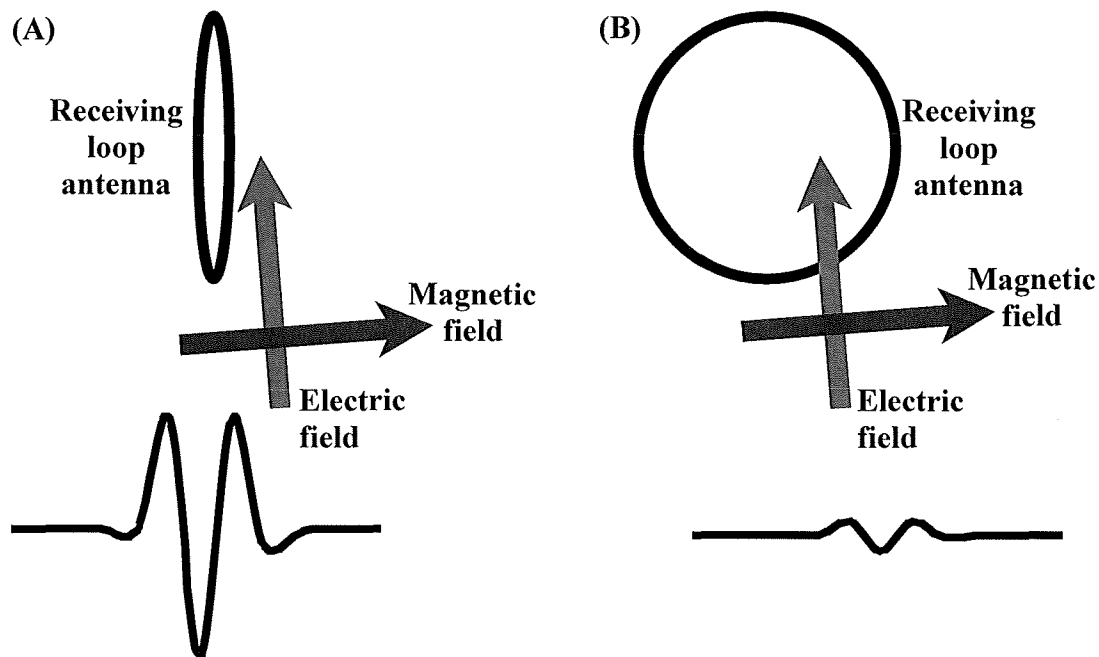


Figure 3. Effect of the orientation of a receiving loop antenna, with respect to an impinging transmitted electromagnetic wave, on the amplitude of the signal induced on the receiving antenna: (A) antenna loop parallel to incident electric field receives the maximum signal amplitude, (B) antenna loop perpendicular to incident electric field receives minimal signal amplitude.

Maximum signal is induced on the antenna when the plane of the loop is parallel to the radial direction to the transmitter. The location of the transmitter is found by determining the radial direction to the transmitter from at least two different locations.

For radar reflection logging, locating the direction to a reflection source is similar to the radio-direction finding problem of locating the direction to a transmitter. In a borehole, however, the direction of movement is limited to the borehole axis, and physical rotation of the antenna is not desirable due to the power demands of a mechanical apparatus. Therefore, specially designed directional antennas are required to determine the strike, dip, and intersection location of planar reflectors, and the azimuth, depth, and radial distance of point reflectors. The directional receiving antenna used for this study is a magnetic dipole tool containing four orthogonal, resistively-loaded, transmission line antennas, which have the same directional radiation properties described for the loop antennas, but with improved signal characteristics (Falk, 1992). The antenna contains a three-component magnetometer and a plunge sensor to determine the orientation of the receiver for each measurement. The four antennas allow the sampling of the spatial components of the reflected electromagnetic waves, without resorting to the

physical rotation of the antennas.

For this study, the commercial software RADINTER was used to interpret the radar reflection logs. RADINTER is an interactive program that allows the user to interpret the projected intersection depth, dip, and strike of planar reflectors and the azimuth to point reflectors. This is done using information on the logging measurement parameters, including distance between the transmitter and receiver, measurement start location, measurement interval, sampling frequency, and average EM propagation velocity (fig. 4). A complete description of the procedures used to interpret the directional data can be found in Falk (1992). Note that the projected intersection depth is relative to the line formed by the axis of the borehole. Therefore, the projected intersection depth can be below the drilled depth of the borehole, in the cased portion of a borehole, or can be negative, which indicates the reflector projects to the borehole axis above the ground surface.

Estimation of Reflector Length

Simple geometric concepts can be used to analyze the planar reflectors observed in radar reflection logs. The simplifications ignore important details such as Fresnel zone and edge effects needed

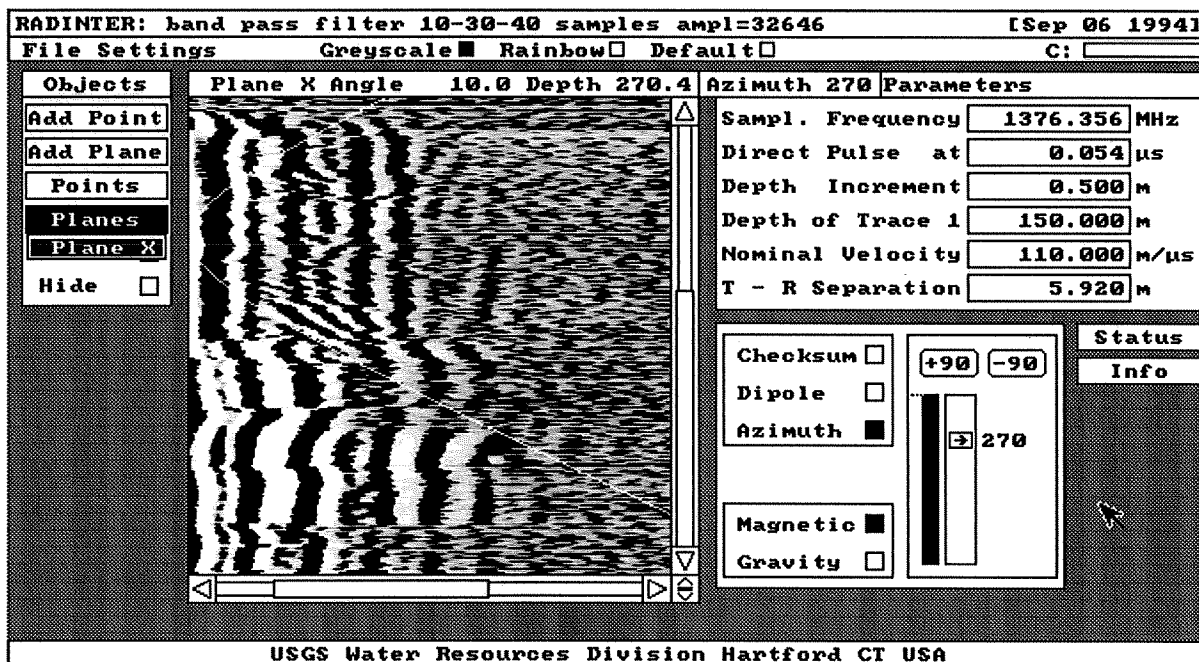


Figure 4. Screen capture showing the use of RADINTER software to interactively interpret borehole-radar reflection logs.

for a more comprehensive analysis; nonetheless, using straight-ray approximations and right-angle trigonometry, useful information about the nature and extent of planar reflectors can be extracted from radar reflection logs. For a thorough discussion of reflection physics, see Yilmaz (1987).

For planar reflectors, the part of the reflector imaged by the logging process is the component parallel to the borehole. Thus, the imaging process is biased by the orientation of the reflector relative to the borehole. For example, the effect of orientation bias on reflectors oriented parallel and perpendicular to the borehole is shown in figure 5. A reflector oriented at a large angle to the borehole reflects EM waves from nearly the same spot as the radar tool is moved along the borehole, whereas for reflectors parallel to the borehole, the imaged spot moves as the radar tool moves (fig. 5). The orientation bias also affects estimates of the location and radial distance to a reflection point; this is similar to the classic migration problem of reflection seismology (Yilmaz, 1987).

Using the geometry shown in figure 5, a reasonable approximation of the radial distance to a point on a reflector is given by

$$D_{\text{cor}} = D_{\text{est}} \cos(\alpha) \quad (1)$$

where

D_{cor} is the corrected radial distance from the borehole,

D_{est} is the estimated distance to reflection point, accounting for fixed transmitter-receiver offset, and

α is the angle of planar reflector to the borehole.

Using this simple radial distance correction, the procedure for calculating the length of a limb of a planar reflector is to (1) use RADINTER to determine the angle of the reflector relative to the borehole; (2) estimate the maximum radial extent of the limb from the reflection record; and (3) correct this distance estimate using equation (1). An estimate of the length of the reflector parallel to the borehole, assuming that the reflector projects close to or intersects the borehole, is given by

$$L_{\text{est}} = D_{\text{cor}} \sin(\alpha) \quad (2)$$

where L_{est} is the estimated length of imaged reflector.

Reflector Quality Scores: Reflector Continuity and Orientation Confidence

The ideal models and simple geometries used to describe theoretical reflection properties often fail to predict real earth reflection characteristics. For example, the ideal planar reflector describes a smooth surface with constant or slowly changing differences in physical properties. In contrast, fracture zones can cross lithologic boundaries; be non-planar; be locally discontinuous; and have abrupt changes in the number, length, and orientation of fractures in the zone. Also, the radar antennas used for this study couple with and are modified by the medium surrounding the antennas. Therefore, real antenna response can and does depart from ideal predicted response.

Because of the differences between ideal and real behavior, a qualitative system of scoring is used to provide a sense of the quality of the data and the confidence in a given interpretation relative to an idealized case. For this study, two scores, ranging from 1 (best) to 5 (worst) are assigned to each reflector for the following categories: (1) reflector continuity and (2) orientation confidence.

The reflector continuity score provides a sense of the spatial persistence of a reflector across the radar reflection log. A score of 1 is assigned to high-amplitude reflectors that originate at or close to the direct wave and are clearly visible with little or no amplitude variations. This type of reflector closely approximates the ideal planar reflector. A reflector continuity score of 3 is assigned to reflectors that show some discontinuity and amplitude variation but can be followed relatively easily across the radar reflection log. This type of reflector is consistent with a locally discontinuous fracture or fracture zone. A reflector continuity score of 5 is assigned to reflectors that are observed in small segments that are isolated and (or) extremely difficult to follow or trace across the radar reflection record. This type of reflector is consistent with isolated, spatially discontinuous fractures and inhomogeneities.

The orientation confidence score provides an indication of the azimuthal (directional) behavior of the reflector relative to the behavior predicted for ideal planar reflectors. The score is also a measure of the confidence of the interpretation. A score of 1 is assigned to reflectors that behave as ideal planar reflectors. A score of 3 is assigned to reflectors that

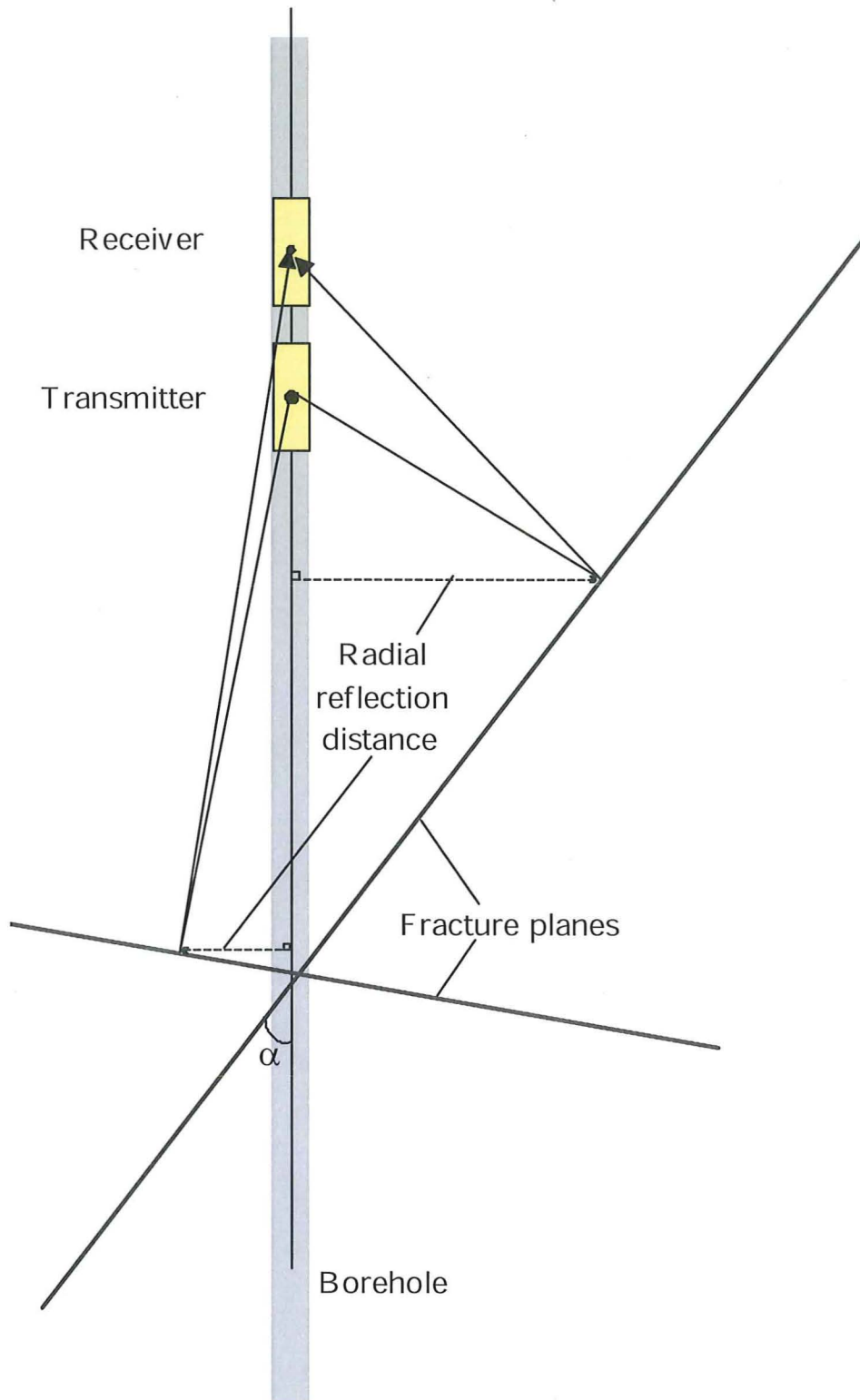


Figure 5. Effect of reflector orientation on reflection imaging.

are partially obscured by other reflectors or where some interference effects are observed but a reasonable interpretation is still possible. These reflectors are consistent with locally discontinuous fractures or fracture zones. A score of 5 is assigned to reflectors that are degraded by severe interference, are difficult to observe at important angles, or are located where the electric-dipole component is missing or obscured. This type of reflector is consistent with chaotic fracture zones or faint reflectors in parts of the reflection record having low signal strength.

RESULTS OF BOREHOLE-RADAR REFLECTION LOGGING AT THE PROJECT SHOAL AREA

Omni-directional and directional-radar reflection logging was conducted using 60-MHz transmitting and receiving antennas in boreholes HC-1, HC-2, HC-5, HC-6, HC-7, and HC-8 at the Project Shoal Area, Churchill County, Nevada (fig. 1). Field logging parameters are listed in table 1. Figures 6 to 10 show (1) processed borehole-radar reflection logs; (2) lower-hemisphere equal-area stereo-nets showing the poles of the radar reflectors weighted by reflector length and combined quality score; and (3) logs showing the results of direct-wave velocity and amplitude analysis. Tables 2-6 give the location, orientation, length, and quality scores for the interpreted reflectors in each borehole.

The quality of the borehole-radar data ranged from very poor to good, with most data in the poor to fair range. Assuming that the radar equipment was functioning properly, the range in data quality can be attributed to the relatively low resistivity of the rocks

underlying the PSA. As electrical resistivity decreases, attenuation of EM waves increases. Therefore, the radial penetration of the radar pulse into the rock is attenuated. In addition, as electrical resistivity decreases, a threshold is reached at which diffusive behavior dominates, and EM-wave propagation is no longer possible. The quality of the radar data collected from borehole HC-1 is so poor that it was uninterpretable; by contrast, the quality of the data from HC-6 and HC-7 was sufficient to map reflectors more than 10 m from the borehole.

Borehole HC-2

Radar reflection logging in borehole HC-2 was limited to omni-directional logging (table 1). Data quality was good (fig. 6A), with radial penetration exceeding 15 m. A total of 8 reflectors were interpreted from the reflection log (table 2). The estimated length of the reflectors imaged in HC-2 ranges from less than 3 m to more than 40 m. Interpreted dips range from about 15 to 80°, with a median dip of 60°. The direct-wave logs indicate the presence of low-velocity zones at depths of about 300 and 335 m (fig. 6B and 6C). Direct-wave amplitude and radial penetration increase below about 330 m, indicating that the electrical resistivity of the rocks below this depth increases.

Borehole HC-5

Radar reflection logging in borehole HC-5 included omni-directional and directional logging (table 1). The quality of the omni-directional and directional radar data was poor (fig. 7A), with few

Table 1. Radar reflection logging parameters, Project Shoal Area, Churchill County, Nevada
[x, data collected; --, no data collected; -, none]

Borehole number	Starting depth (meters)	Stopping depth (meters)	Step (meters)	Sampling frequency (megahertz)	Directional data collected	Omni-directional data collected	Comments
HC-1	339.25	400.00	0.25	1605.73	--	x	uninterpretable
HC-2	294.00	367.00	0.50	719.43	--	x	-
HC-5	390.00	592.00	0.50	917.60	x	x	-
HC-6	229.00	360.00	0.50	1376.36	x	x	-
HC-7	139.00	366.50	0.50	1310.82	x	x	-
HC-8	394.00	742.00	0.50	917.60	x	x	-

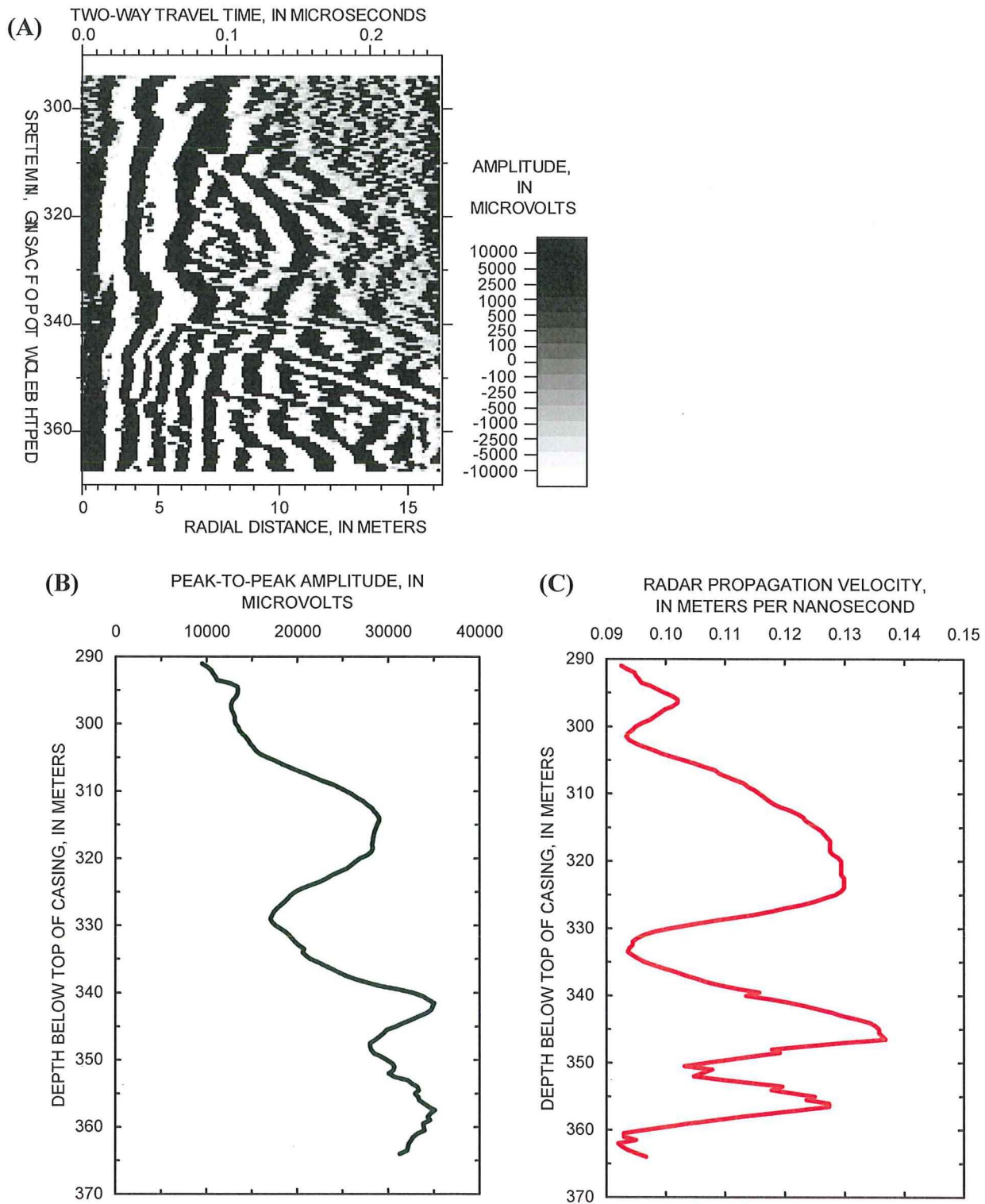


Figure 6. Radar reflection logging in borehole HC-2, Project Shoal Area, Churchill County, Nevada: (A) 60-megahertz electric-dipole omni-directional radar reflection log, (B) direct-wave amplitude log, (C) direct-wave radar velocity log.

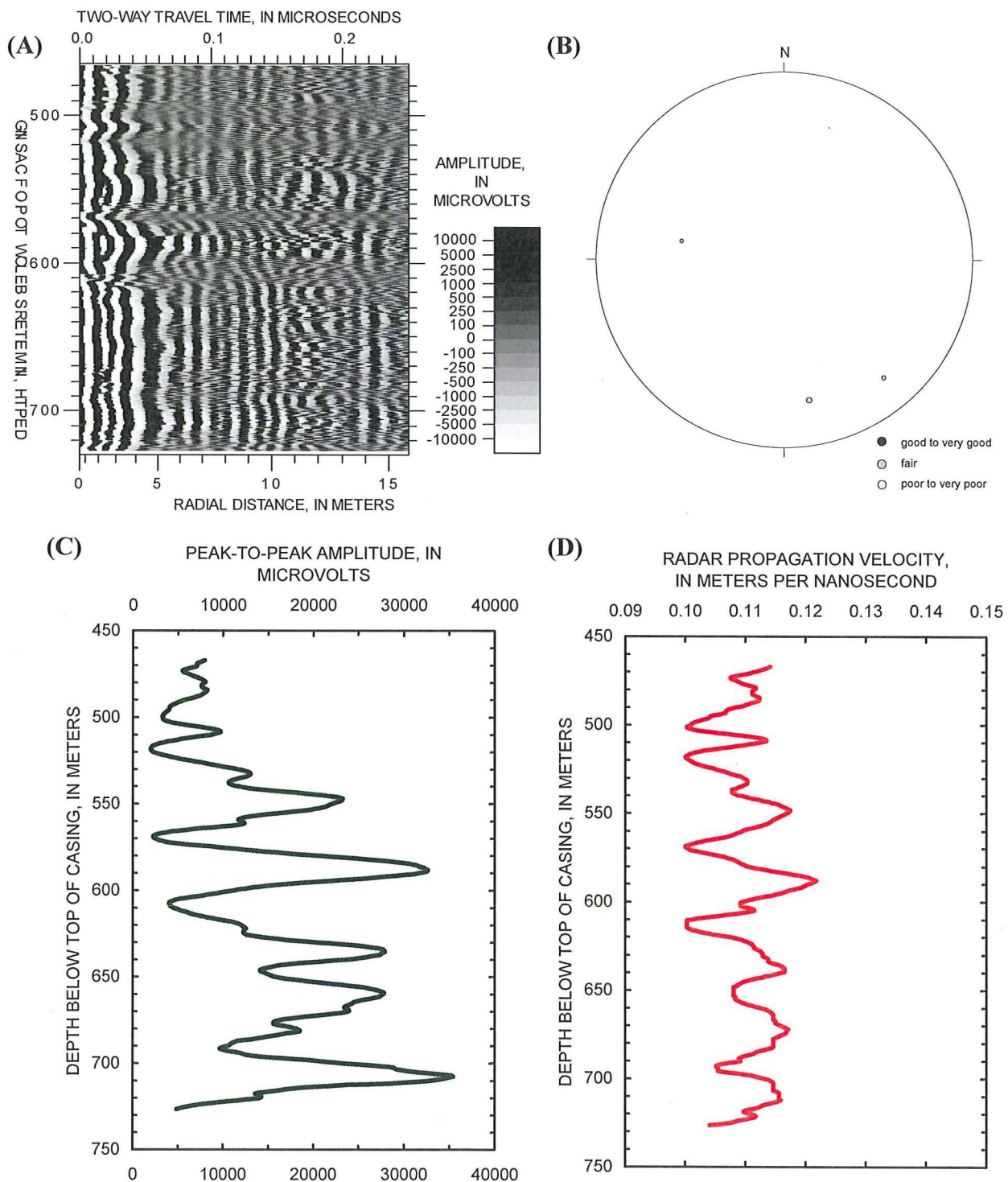


Figure 7. Radar reflection logging in borehole HC-5, Project Shoal Area, Churchill County, Nevada: (A) 60-megahertz magnetic-dipole directional radar reflection log, (B) lower hemisphere equal-area stereo-net showing poles of interpreted reflectors, (C) direct-wave amplitude log, (D) direct-wave radar velocity log.

Table 2. Planar reflectors interpreted from 60-megahertz radar reflection log, borehole HC-2, Project Shoal Area, Churchill County, Nevada

Depth from land surface (meters)	Dip (degrees)	Reflector continuity (1 = very good, 5 = very poor)	Estimated length of reflector (meters)	Comments
284.5	78	2	42.0	lower limb
299.5	62	4	24.0	lower limb
312.5	61	3	18.7	lower limb
318.5	52	4	8.7	lower limb
332.5	52	1	19.7	lower limb
333.2	15	3	2.6	lower limb
340.5	60	4	16.7	lower limb
354.4	60	5	8.7	lower limb

interpretable reflectors. Three reflectors were interpreted from the directional reflection log (table 3). Two reflectors strike west to southwest, dipping between 65 and 70°, one reflector strikes 10° east of north with a dip of 46°. These data are plotted on a pole-plane stereonet (fig. 7B). Each reflector is symbolized as a pole to the reflector plane, projected onto a lower-hemisphere, equal-area stereonet. The estimated length of the reflectors imaged in HC-5 ranges from less than 7 m to more than 40 m. The direct-wave logs indicate the presence of several minor low-velocity zones at depths of about 500, 520, 570, and 620 m. Direct-wave amplitudes generally increase with depth except near the low-velocity zones (figs. 7C and 7D).

Borehole HC-6

Radar reflection logging in borehole HC-6 included omni-directional and directional logging (table 1). The quality of the omni-directional and

directional radar data was fair to good (fig. 8A). Five reflectors were interpreted from the directional reflection log (table 4). One reflector strikes to the northwest with a dip of 83°. Two reflectors strike southwest dipping at 71 and 80°, and two reflectors strike southeast with dips of 63 and 73°, respectively (fig. 8B). The median dip of the interpreted reflectors is 73°. The estimated length of the reflectors imaged in HC-6 ranges from less than 15 m to more than 140 m; the median reflector length is 37 m. The direct-wave logs indicate the presence of low-velocity zones above 100 m and below 300 m. An isolated low-velocity zone occurs at about 165 m. Direct-wave amplitudes generally increase with depth. The lowest direct-wave amplitudes occur above 100 m; amplitudes are fairly constant from 100 to 300 m except near the low velocity zone at 165 m (figs. 8C and 8D). It is interesting to note that direct-wave amplitudes increase below 300 m, whereas direct-wave velocities decrease over the same interval. This suggests that an increase in primary or secondary

Table 3. Planar reflectors interpreted from 60-megahertz radar reflection log, borehole HC-5, Project Shoal Area, Churchill County, Nevada

Depth from land surface (meters)	Strike (degrees)	Dip (degrees)	Reflector continuity (1=very good, 5=very poor)	Orientation confidence (1=very good, 5=very poor)	Estimated length of reflector (meters)	Comments
448.1	260	65	4	4	41.5	upper limb
464.2	230	70	4	4	21.0	upper limb
482.7	10	46	3	5	6.6	lower limb

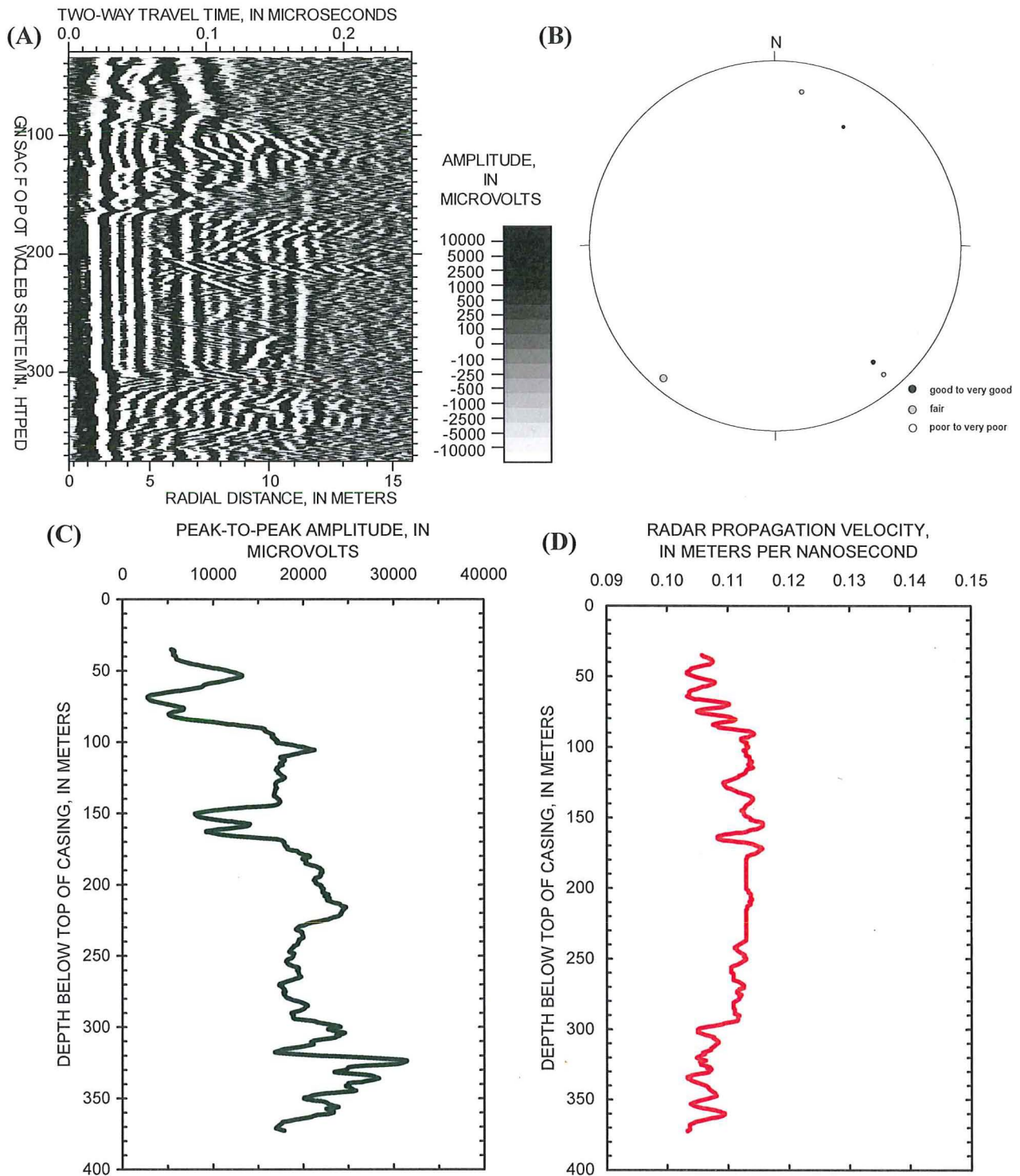


Figure 8. Radar reflection logging in borehole HC-6, Project Shoal Area, Churchill County, Nevada: (A) 60-megahertz magnetic-dipole directional radar reflection log, (B) lower hemisphere equal-area stereo-net showing poles of interpreted reflectors, (C) direct-wave amplitude log, (D) direct-wave radar velocity log.

Table 4. Planar reflectors interpreted from 60-megahertz radar reflection log, borehole HC-6, Project Shoal Area, Churchill County, Nevada

Depth from land surface (meters)	Strike (degrees)	Dip (degrees)	Reflector continuity (1=very good, 5=very poor)	Orientation confidence (1=very good, 5=very poor)	Estimated length of reflector (meters)	Comments
218.0	310	83	3	4	147.8	lower limb
257.7	120	63	3	3	14.4	crossing
270.4	230	80	4	4	34.7	crossing
271.6	230	71	2	3	34.5	lower limb
332.7	100	73	4	3	40.0	upper limb

porosity associated with a decrease in specific conductance of the ground water and (or) a change in mineral assemblage, is taking place in the rocks below 300 m.

Borehole HC-7

Radar reflection logging in borehole HC-7 included omni-directional and directional logging (table 1). The quality of the omni-directional and directional radar data was fair to good (fig. 9A). Fourteen reflectors were interpreted from the directional reflection log (table 5). The reflectors are clustered in three groups: (1) a northwest-southeast striking set with dips ranging from 73 to 84°; (2) an east-west striking set with dips ranging from 80 to 87°; and (3) a northeast-southwest striking set with dips ranging from 69 to 86° (fig. 9B).

The estimated length of the reflectors imaged in HC-7 ranges from less than 18 to more than 130 m; the median reflector length is 50 m. The direct-wave amplitude logs from HC-7 are remarkably similar to the logs from HC-6, when shifted upward 50 m. The direct-wave logs indicate that a continuous structure or structures could connect boreholes HC-6 and HC-7. The lowest velocities are present above 120 m and below 300 m. Isolated low-velocity zones occur at about 185 and 225 m. As in HC-6, direct-wave amplitudes generally increase with depth. The lowest

direct-wave amplitudes occur above 120 m; amplitudes are fairly constant from 120 to 270 m except near the low-velocity zone at 220 m (figs. 9C and 9D). As in HC-6, direct-wave amplitudes increase below 300 m over the same interval that direct-wave velocities decrease, indicating an increase in primary or secondary porosity coupled with a decrease in the specific conductance of ground water, and (or) a change in mineral assemblage.

Borehole HC-8

Radar reflection logging in borehole HC-8 included omni-directional and directional logging (table 1). The quality of the omni-directional and directional radar data was fair (fig. 10A). Five reflectors were interpreted from the directional reflection log (table 6). All of the reflectors have strikes near north-south with dips ranging from 56 to 71° with a median dip of 63° (fig. 10B). The estimated length of the reflectors imaged in HC-8 ranges from less than 15 to about 28 m, the median reflector length is 19 m. The direct-wave logs indicate the presence of low-velocity zones near 630 and 710 m. Additional isolated low-velocity zones occur at about 655 and 665 m. Direct-wave amplitudes are generally constant over the logged interval except for decreases near the low-velocity zones (figs. 10C and 10D).

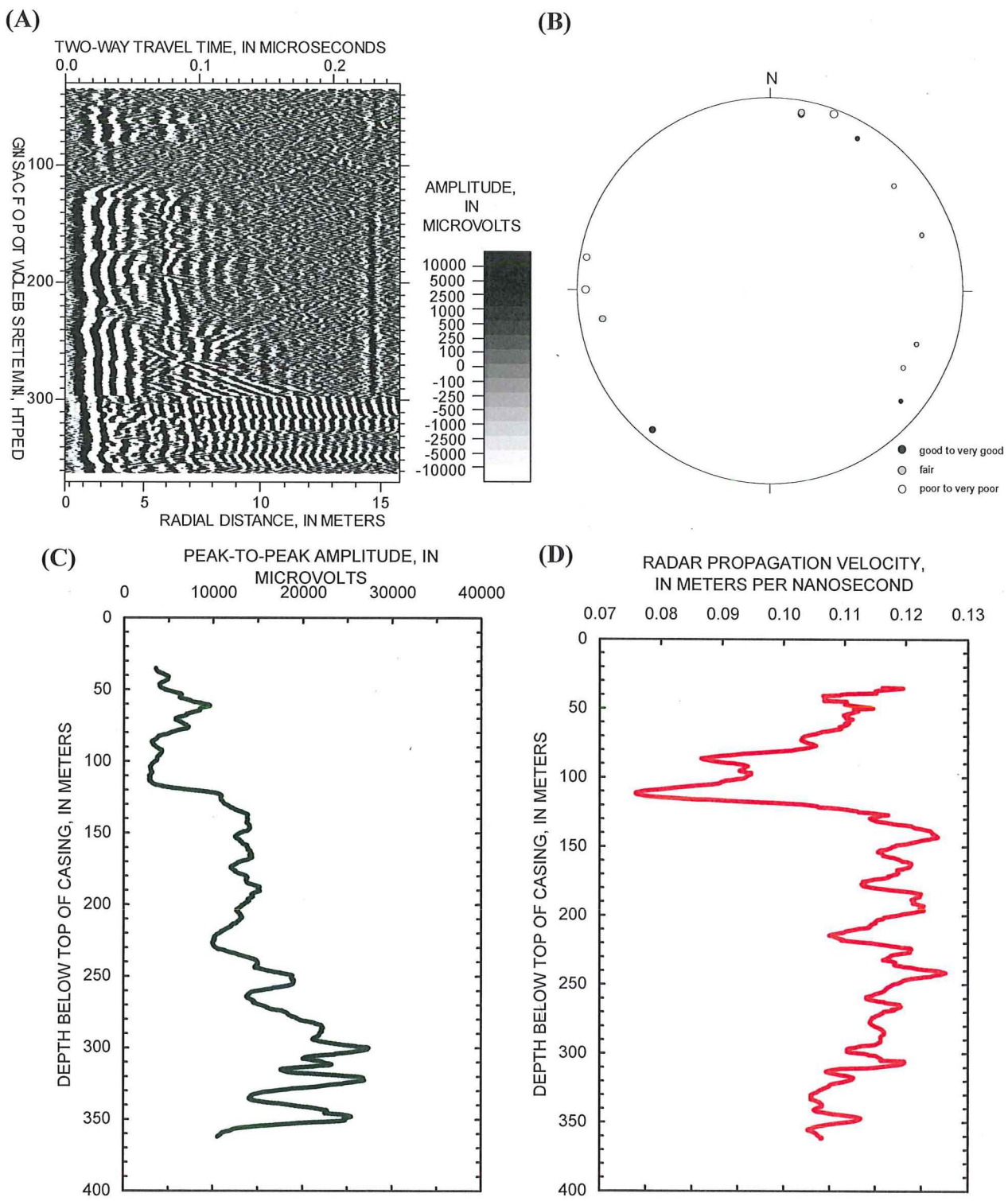


Figure 9. Radar reflection logging in borehole HC-7, Project Shoal Area, Churchill County, Nevada: (A) 60-megahertz magnetic-dipole directional radar reflection log, (B) lower hemisphere equal-area stereo-net showing poles of interpreted reflectors, (C) direct-wave amplitude log, (D) direct-wave radar velocity log.

Table 5. Planar reflectors interpreted from 60-megahertz radar reflection log, borehole HC-7, Project Shoal Area, Churchill County, Nevada
 [n/a, not applicable - represents dipole only]

Depth from land surface (meters)	Strike (degrees)	Dip (degrees)	Reflector continuity (1=very good, 5=very poor)	Orientation confidence (1=very good, 5=very poor)	Estimated length of reflector (meters)	Comments
206.6	0	85	5	5	121.6	lower limb
219.7	10	86	5	5	80.1	lower limb
228.0	220	78	2	4	39.4	lower limb
282.7	200	70	3	4	32.6	crossing
310.4	160	73	4	4	32.7	crossing
318.6	n/a	74	5	5	17.5	lower limb
329.1	100	82	2	2	72.1	lower limb
340.1	100	83	3	4	60.8	lower limb
364.2	120	80	3	2	40.1	lower limb
424.9	310	84	3	2	80.2	upper limb
426.1	350	77	4	4	63.5	crossing
451.4	140	73	4	5	29.1	upper limb
468.2	210	69	5	4	21.3	upper limb
540.2	110	87	4	5	133.6	upper limb

Table 6. Planar reflectors interpreted from 60-megahertz radar reflection log, borehole HC-8, Project Shoal Area, Churchill County, Nevada

Depth from land surface (meters)	Strike (degrees)	Dip (degrees)	Reflector continuity (1=very good, 5=very poor)	Orientation confidence (1=very good, 5=very poor)	Estimated length of reflector (meters)	Comments
381.7	350	56	5	5	28.3	lower limb
406.8	170	63	5	5	14.2	lower limb
419.9	190	71	2	4	18.3	lower limb
426.6	190	58	3	4	19.4	crossing
434.6	180	63	4	4	23.6	crossing

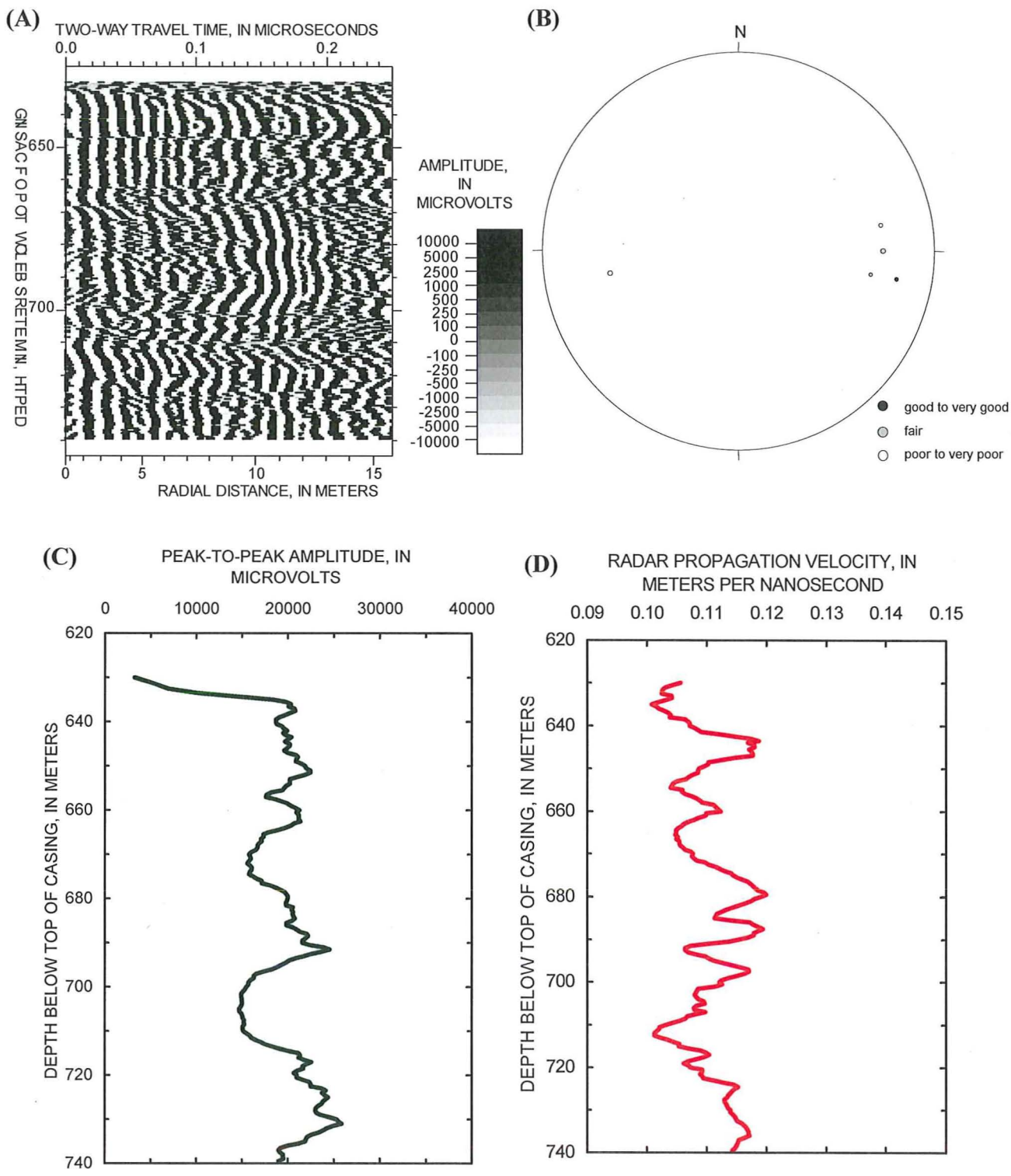


Figure 10. Radar reflection logging in borehole HC-8, Project Shoal Area, Churchill County, Nevada: (A) 60-megahertz magnetic-dipole directional radar reflection log, (B) lower hemisphere equal-area stereo-net showing poles of interpreted reflectors, (C) direct-wave amplitude log, (D) direct-wave radar velocity log.

SUMMARY AND CONCLUSIONS

Borehole-radar reflection logging using 60-MHz omni-directional and directional antennas was conducted at the Project Shoal Area, Churchill County, Nevada. The overall quality of the radar data is marginal, ranging from very poor to good. Six boreholes were logged (HC-1, HC-2, HC-5, HC-6, HC-7, and HC-8), but the data from one borehole (HC-1) were uninterpretable. Of the five boreholes interpreted, four (HC-5, HC-6, HC-7, and HC-8) were logged using a directional receiving antenna capable of providing the information to determine the reflector orientation.

Twenty-seven reflectors were interpreted from the directional radar reflection logs. Histograms summarizing the range of interpreted azimuths (strike) and dips are shown in figures 11 and 12. Azimuths are concentrated in two orientations — northeast-southwest and east-west to slightly northwest-southeast. Reflectors are moderate to steeply dipping. The mean reflector dip is 72.6° ; the median is 73° with a standard deviation of 10.1° . Reflector length was estimated for each reflector using a straight-ray reflection path approximation. Reflector length ranged from less than 7 to more than 133 m, with a mean of 47 m, median of 34.5 m, and standard deviation of 37.3 m.

Reflector quality scores from 1 (best) to 5 (worst) were assigned to each reflector to provide a sense of the spatial continuity of the reflectors and the comparison of the field data relative to an ideal planar reflector. The average reflector continuity score is 3.6 (fair to poor range, fig. 13), consistent with fractures or fracture zones that contain localized to moderate discontinuities but which are still relatively continuous over a scale of tens of meters.

The orientation confidence scores are low, generally about 4.0 (fig. 14). The low scores reflect

the general data quality, but also indicate that the behavior of most reflectors departs from the ideal planar case. The low scores are consistent with reflections from fracture zones containing numerous, closely spaced, sub-parallel fractures.

An equal-area stereo-net that summarizes interpretations from all of the boreholes logged at the PSA is shown in figure 15. In general, the most continuous reflectors are those having the steepest dips, and either north-south or east-west strikes.

Direct-wave analysis performed on the radar reflection logs was used to generate logs of radar velocity and amplitude. Zones of low radar velocity correlate with decreases in direct-wave amplitude, most likely indicating the presence of saturated fracture zones. In boreholes HC-5, HC-6, and HC-7, direct-wave amplitudes increase with depth; this suggests an overall increase in electrical resistivity, possibly due to changes in mineral assemblage and (or) to a decrease in the specific conductance of ground water. In boreholes HC-6 and HC-7, at depths below 300 m, the direct-wave amplitudes increase over the same interval where direct-wave velocities are decreasing. This observation is consistent with an increase in primary or secondary porosity coupled with a decrease in specific conductance of ground water, and (or) a change in mineral assemblage. Another observation is the similarity between the direct-wave logs from HC-6 and HC-7 when the HC-7 log is shifted upward about 50 m. The similarities suggest that HC-6 and HC-7 are connected by structural features with a down-dip component in the direction of HC-7. The results of the borehole-radar reflection logging indicate that even where data quality is marginal, these data can provide useful information for ground-water characterization studies in fractured rock, and provide insights into the nature and extent of fractures and fracture zones in and near boreholes.

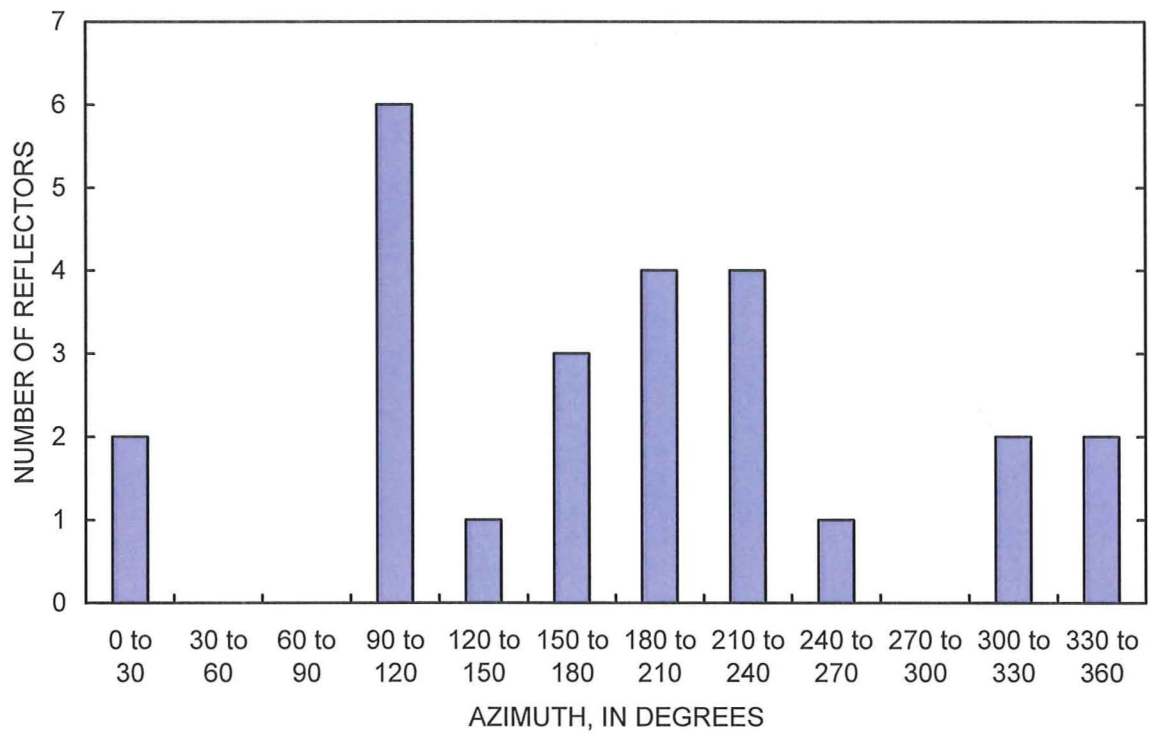


Figure 11. Distribution of interpreted borehole-radar reflectors sorted by azimuth, Project Shoal Area, Churchill County, Nevada.

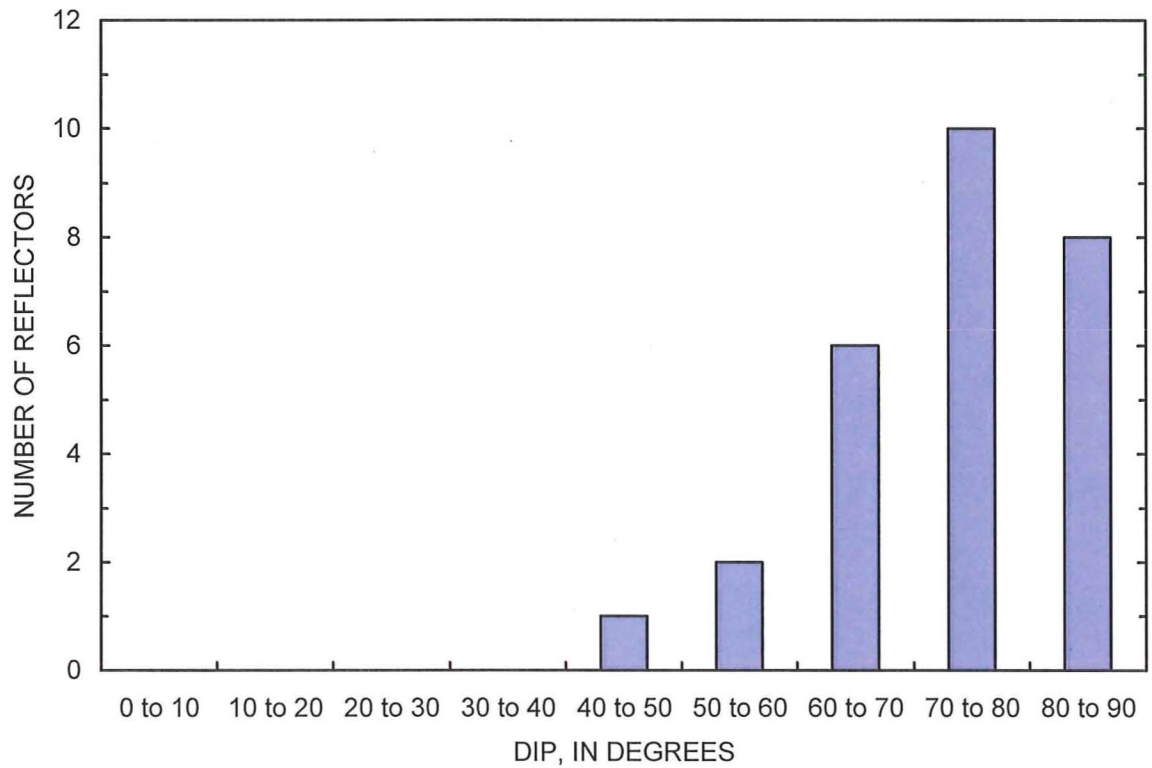


Figure 12. Distribution of interpreted borehole-radar reflectors sorted by dip, Project Shoal Area, Churchill County, Nevada.

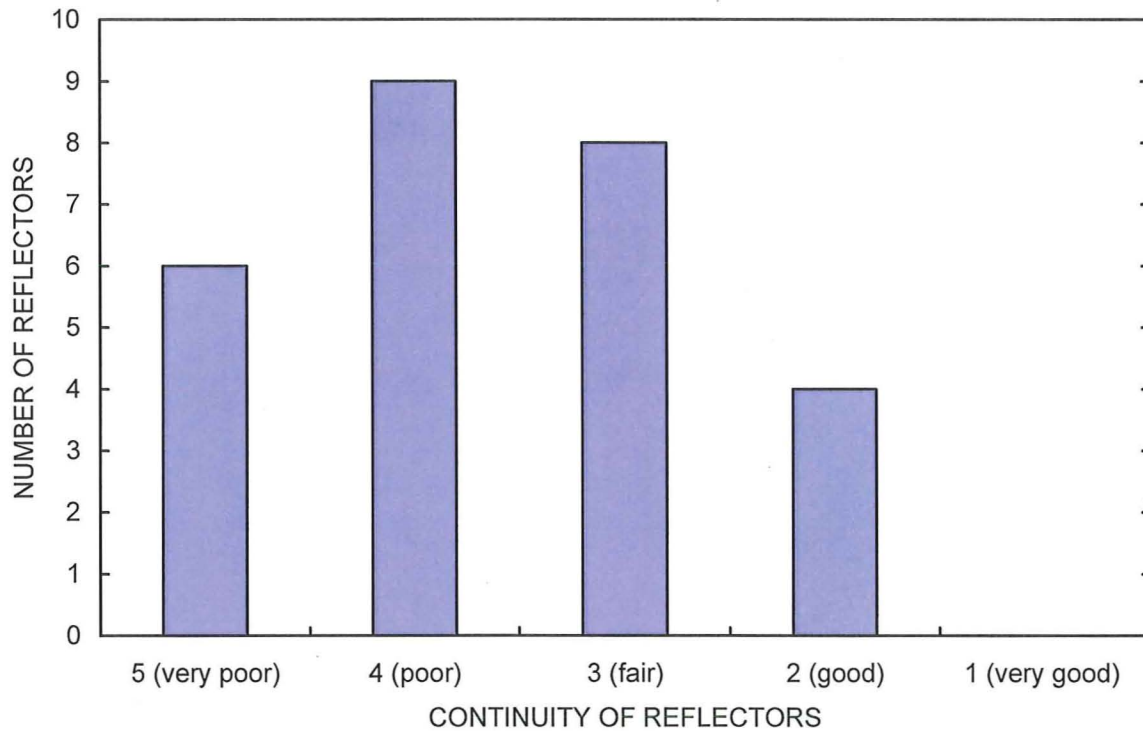


Figure 13. Distribution of interpreted borehole-radar reflectors sorted by the continuity of the reflectors, Project Shoal Area, Churchill County, Nevada.

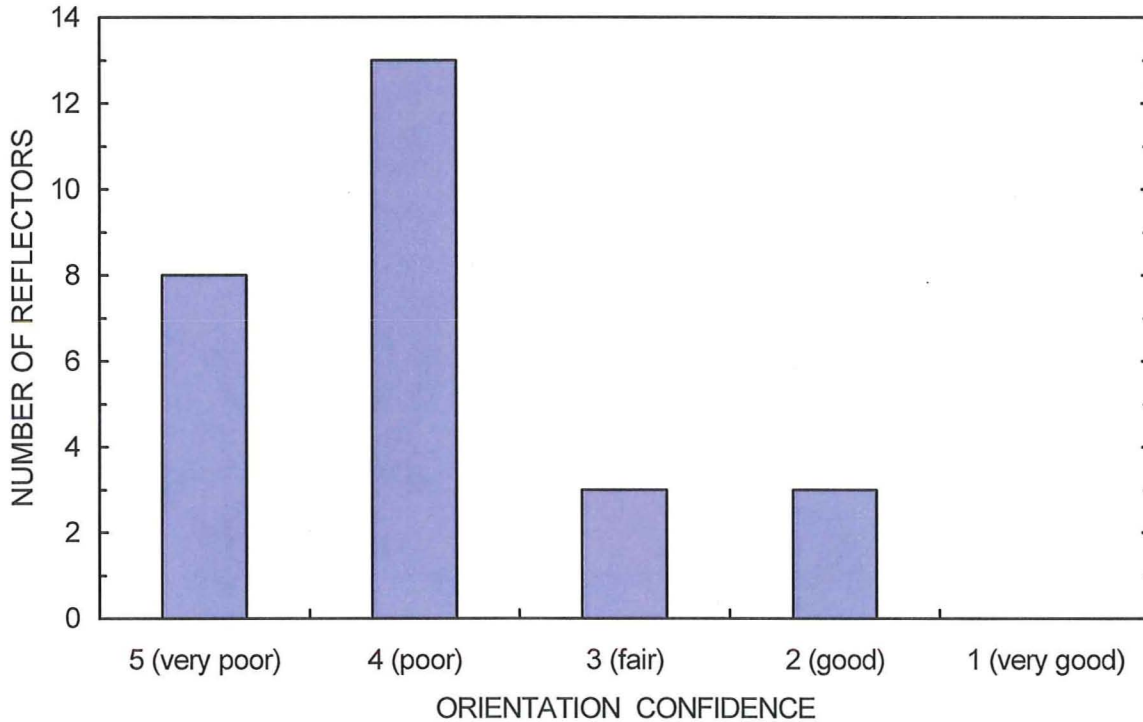


Figure 14. Distribution of interpreted borehole-radar reflectors sorted by orientation confidence, Project Shoal Area, Churchill County, Nevada.

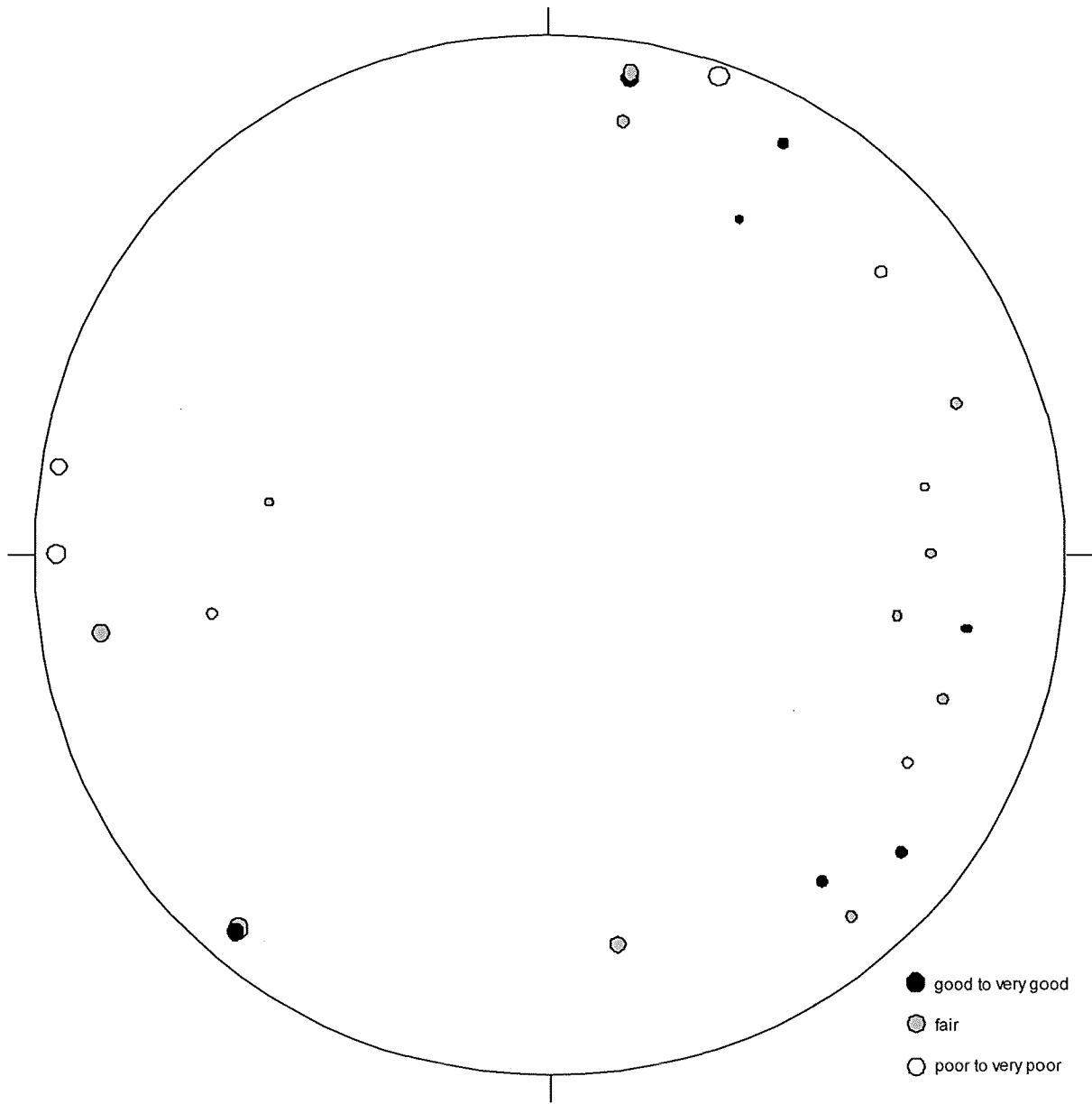


Figure 15. Lower hemisphere equal-area stereo-net showing poles of all interpreted radar reflectors, weighted by reflector length and combined reflector quality, Project Shoal Area, Churchill County, Nevada.

REFERENCES CITED

- Bradley, J.A., and Wright, D.L., 1987, Microprocessor-based data-acquisition system for a borehole radar: *IEEE Transactions on Geosciences and Remote Sensing*, GE-24, p. 441-447.
- Cohen, P., and Everett, D., 1963, A brief appraisal of the ground-water hydrology of the Dixie-Fairview Valley area, Nevada: Carson City, Nevada, Department of Conservation and Natural Resources, Ground-Water Resources Reconnaissance Series, v. 23, 40 p.
- Cook, J.C., 1975, Radar transparencies of mine and tunnel rocks: *Geophysics*, v. 40, no. 5, p. 865-885.
- Falk, L., 1992, Directional borehole antenna--theory, Stripa Project 92-16, SKB: Stockholm, Sweden, 138 p.
- Gaylor, R., Liebllich, D.A., Mariani, D., and Xia, J., 1994, Environmental logging with a borehole radar tool, *in* Proceedings of the Second International Conference on Ultra-Wideband Short-Pulse Electromagnetics, April 5-7: New York, New York Polytechnic University, 20 p.
- Glancy, P. and Katzer, D., 1975, Water resources appraisal of the Carson River Basin, Western Nevada: Carson City, Nevada, Department of Conservation and Natural Resources, Water Resources-Reconnaissance Series, v. 59, 126 p.
- Haeni, F.P., Lane, J.W., Jr., and Liebllich, D.A., 1993, Use of surface-geophysical and borehole-radar methods to detect fractures in crystalline rocks, Mirror Lake area, Grafton County, New Hampshire *in* Banks, S., and Banks, D., (eds.) Hydrogeology of Hard Rocks: Memoires of the 24th Congress--International Association of Hydrogeologists, v. 29, part 1, June 28-July 2, Oslo, Norway, 11 p.
- Hansen, B.P., and Lane, J.W., Jr., 1995, Use of surface and borehole geophysical surveys to determine fracture orientation and other site characteristics in crystalline bedrock terrain, Millville and Uxbridge, Massachusetts: U.S. Geological Survey Water-Resources Investigations Report 95-4121, 25 p.
- Holloway, A.L., Stevens, K.M., and Lodha, G.S., 1992, The results of surface and borehole radar profiling from permit area B of the Whiteshell Research Area, Manitoba, Canada, *in* Hanninen, Pauli and Autio, Sini (eds.), Fourth International Conference on Ground Penetrating Radar: Geological Survey of Finland Special Paper 16, p. 329-337.
- Lane, J.W., Jr., Haeni, F.P., and Williams, J.H., 1994, Detection of bedrock fractures and lithologic changes using borehole radar at selected sites, *in* Fifth International Conference on Ground-Penetrating Radar (GPR '94), Kitchener, Ontario, Canada, June 12-16, 1994, Proceedings: Kitchener, Ontario, Canada, p. 577-592.
- Nilsson, B., 1983, A new borehole radar system, *in* Proceedings of the KEGS symposium on borehole geophysics--mining and geotechnical applications: Toronto, Canada, 400 p.
- Olsson, O., Andersson, P., Carlsten, S., Falk, L., Niva, B., and Sandberg, E., 1988, Fracture characterization in crystalline rock by borehole radar: Workshop on Ground-Penetrating Radar, May 24-26, Ottawa, Canada, 24 p.
- Olsson, O., Anderson, P., Carlsten, S., Falk, L., Niva, B., and Sandberg, E., 1992a, Fracture characterization in crystalline rock by borehole-radar, *in* Pilon, J., ed., Ground-Penetrating Radar: Geological Survey of Canada Paper 90-4, p. 139-150.
- Olsson, O., Falk, L., Forslund, O., Lundmark, L., and Sandberg, E., 1992b, Borehole radar applied to the characterization of hydraulically conductive fracture zones in crystalline rock: *Geophysical Prospecting*, v. 40, p. 109-142.
- Pohll, G., Chapman, J., Hassan, A., Papelis, C., Andricevic, R., and Shirley, C., 1998, Evaluation of groundwater flow and transport at the Shoal underground nuclear test - an interim report: Desert Research Institute Water Resources Center Publication No. 45162, 123 p.
- Rubin, L.A., Fowler, J.C., and Marino, G.G., 1978, Borehole radar: Springfield, Virginia, Ensco Project 114.
- Sandberg, E.V., Olsson, O. L., and Falk, L. R., 1991, Combined interpretation of fracture zones in crystalline rock using single-hole, crosshole tomography, and directional borehole-radar data: *The Log Analyst*, v. 32, no. 2, p. 108-119.
- Stevens, K.M., Lodha, G.S., Holloway, G.S., and Soonawala, N.M., 1995, The application of ground penetrating radar for mapping fractures in plutonic rocks within the Whiteshell Research area, Pinewa, Manitoba, Canada: *Applied Geophysics*, v. 33, no. 1-3, p. 125-143.

- University of Nevada, 1965, Geological, geophysical, chemical, and hydrological investigations of the Sand Springs Range, Fairview Valley, and Fourmile Flat, Churchill County, Nevada: U.S. Atomic Energy Commission, Vela Uniform Report, v. 1001, 369 p.
- Wright, D.L., and Watts, R. D., 1982, A single-hole, short-pulse radar system, *in* Geophysical Investigations in Connection with Geological Disposal of Radioactive Waste: Ottawa, Canada, OECD/NEA, 317 p.
- Yilmaz, Özdođan, 1987, Seismic data processing, *in* Investigations in Geophysics: Tulsa, Oklahoma, Society of Exploration Geophysics, v. 2, 526 p.